Angular Distribution of Radiation Reflected from Roughened Spheres

D. C. Look*
University of Missouri – Rolla, Rolla, Mo.
and
B. W. Rau†
DuPont Chemical Co., Seaford, Del.

Introduction

THIS Note is concerned with four models for nonregular reflection from a flat plate: Lambert, Lommel-Seeliger, Euler, and the shape factor. A complete bibliography of reflectance from surfaces has been compiled by Rau and Look.[1] This compilation includes the efforts of Russell[2] and Schoenberg[3] who investigated reflection from spheres using three of the aforementioned models. The fourth model is the result of an investigation[4] whose aim was to deduce an expression that closely agreed with the experimental data of light reflected from a flat surface of pressed aluminum oxide.

For the four analyses, based on the flat plate engineering intensity, equations were deduced for the radiometric intensity, the flux, and the power reflected from a roughened sphere. An experiment was then performed to obtain a limited amount of data descriptive of the radiant power bidirectionally reflected from four samples of nonregularly reflecting white spheres. The data was then compared to the four models to determine which model's theoretical results best fit the experimental data.

Analysis

In the spatial geometry utilized, ψ is the polar angle the collimated incident radiation makes with the average surface normal, whereas θ is the polar angle to the detector. β is the included angle between the incident and the reflected directions, with Φ the azimuthal angle in the plane of the surface.

Table 1 may be used to compare the four reflection analyses results. This table was developed using the following definitions

Monospectral engineering flux

$$F_\nu = Q_\nu / A = \int_\omega I_\nu \cos\gamma \mathrm{d}\omega \tag{1}$$

Radiometric intensity

$$I_{R_\nu} = Q_\nu / \omega = \int_A I_\nu \cos\gamma \mathrm{d}A \tag{2}$$

Reflected intensity

$$I_\nu = 1/\pi \int_\omega f_\nu(\upsilon, \zeta, \tau, \theta, \phi, \psi)\ I'_\nu \cos\psi \mathrm{d}\omega' \tag{3}$$

where γ may be either ψ or θ, ω is the solid angle, A is the area, f_ν is the reflection function, and the primed variables indicate incident quantities.

It follows directly that the monospectral power is both

$$Q_\nu = \int_A F_\nu \mathrm{d}A$$

and

$$Q_\nu = \int_\omega I_R \mathrm{d}\omega \tag{4}$$

The assumptions for these calculations are that the intensities presented in the first column are given, the reflection functions are constant ($f_\nu = R_\nu$), and the sphere is composed of an infinite number of flat plates (ψ and θ are different for each of them). In Table 1, the coefficients of the expressions are normalized, for convenience, by letting $4R_\nu F'_\nu a^2 \Delta\omega / 3\pi = 1$, in which a is the radius of the sphere.

Instrumentation and Specimen Characteristics

The device used to acquire data is shown schematically in Fig. 1. The source, S (a 150-W tungsten filament lamp) is diffused by frosted glass and focused through a small opening to produce essentially a point source. Mirror, M_1, collects and collimates the light from this source. The large rotatable arm carries the source, source optics, and independently rotatable specimen mount (its axis of rotation is also through the apex of the angle, β).

At point T, the spheres are mounted on a black cone-shaped holder. The light that irradiates a hemisphere is not incident upon the mount because of a baffled enclosure about the light source that prevents it. As the spheres are interchanged in the experiment, the mount was raised and lowered so that the plane between M_1, M_2 and the center of the spheres remains the same.

The reflected power scattered at angle β is collected and refocused by M_2 to the aperture slit of a spectrometer, D (adjusted to detect the radiant energy about $0.49 \pm 0.02\mu$). The off-axis parabolic, first surface mirrors, M_1 and M_2, are 4.25 in. diam with a focal length of 43 in. The voltage drop across the photomultiplier load resistor was recorded as a function of β. Voltage measurements were made by means of a multirange voltmeter, which has a calibrated accuracy and a departure from linearity of 1%/h.

Three of the four spheres used were clear acrylic plastic (diameters of 2, 2.5, and 3 in.). The fourth was of 1.75-in.-diam cream-colored nylon. All of the spheres were peened with fine glass beads such that the overall shape was not distorted. All spheres were then spray-painted several times with Eastmen White Reflectance Paint until they were opaque.

To be certain that the reflection characteristics of the spheres were isotropic, they were viewed while rotating about the vertical axis at point T. This test indicated that there was essentially no variation in the power reflected as the spheres were rotated about this axis.

Data Acquisition and Reduction Procedure

A cathometer was used to align the center of the sphere at axis T and be sure that M_1, M_2 and the center of the sphere were in the same horizontal plane. Next the large arm was rotated to $\beta = 15°$. The power reading on a digital voltmeter was then recorded. The angle β was increased in 5° increments and power readings recorded until the value of the reflected power reading was below 0.09 mV where data acquisition was terminated. Figure 2 illustrates the data.

The power received may be represented by the equation

$$V_i = V_0 + V_d \overline{F}$$

in which V_i is the received power (millivolts) as a function of β, V_0 (the dark level – this factor will account for stray

Presented as Paper 75-666 at the AIAA 10th Thermophysics Conference, Denver, Colo., May 27-29, 1975; submitted Aug. 4, 1976; revision received Sept. 20, 1976.
Index category: Radiation and Radiative Heat Transfer.
*Associate Professor, Thermal Radiative Transfer Group, Mechanical and Aerospace Engineering Dept. Member AIAA.
†R&D Engineer, Textile Fiber Division.

Table 1 Normalized radiative heat transfer quantities

Model	I, $(\frac{W}{cm^2\,steradian})$	F, $(\frac{W}{cm^2})$	I_R, $(\frac{W}{steradian})$	Power, Q (W)
Lambert	$\frac{3\cos\psi}{4\Delta\omega a^2}$	$\frac{3\cos\psi\cos\theta}{4a^2}$	$\frac{1}{2\Delta\omega}[(\pi-\beta)\cos\beta+\sin\beta]$	$\frac{1}{2}[(\pi-\beta)\cos\beta+\sin\beta]$
Lommel-Seeliger	$\frac{3\cos\psi}{4\Delta\omega a^2(\cos\psi+\cos\theta)}$	$\frac{3\cos\psi\cos\theta)}{4a^2(\cos\psi+\cos\theta)}$	$\frac{3\pi}{8\Delta\omega}\int_{\beta-\pi/2}^{\pi/2}\frac{\cos\phi\cos\beta+\sin\phi\sin\beta}{1+\cos\beta+\tan\phi\sin\beta}d\phi$	$\frac{3\pi}{8}\int_{\beta-\pi/2}^{\pi/2}\frac{\cos\phi\cos\beta+\sin\phi\sin\beta}{1+\cos\beta+\tan\phi\sin\beta}d\phi$
Euler	$\frac{3\cos\psi}{4\Delta\omega a^2\cos\theta}$	$\frac{3\cos\psi}{4a^2}$	$\frac{3\pi\cos^2(\beta/2)}{4\Delta\omega}$	$\frac{3\pi\cos^2(\beta/2)}{4}$
s factor	$\frac{3\cos^s\psi}{4\Delta\omega a^2}\left(\frac{\cos\theta}{\cos^2(\beta/2)}\right)^{s-1}\frac{3\cos^s\psi\cos^s\theta}{4a^2(\cos^2\beta/2)^{s-1}}$		$\frac{3\Gamma(s+1)\sqrt{\pi}}{4\Delta\omega[\cos^2\beta/2]^{s-1}\Gamma(s+3/2)}\times\int_{\beta-\pi/2}^{\pi/2}\cos^s\phi\cos^s(\phi-\beta)d\phi$	$\frac{3\Gamma(s+1)\sqrt{\pi}}{4[\cos^2\beta/2]^{s-1}\Gamma(s+3/2)}\times\int_{\beta-\pi/2}^{\pi/2}\cos^s\phi\cos^s(\phi-\beta)d\phi$

radiation), and V_d (a constant). $\bar{F}$ is different for each analysis and is the function listed in the fourth column of Table 1. Therefore, the input data to be reduced using a one-shot method of least squares were a series of (V_i, β_i) pairs resulting in V_0 and V_d values for each of the four analyses.

For the s-factor analysis, the determination of s was made statistically. Because of this, the s-factor analysis program was not terminated with the computation of V_d and V_0 as was the case with the other three analyses. That is, alternate computations of (V_d, V_0) pairs and s-factors were made until the variance was minimized.

Discussion of Results

Some of the results of the reductions of the data are presented in Figs. 3 and 4 (both are illustrations of percent deviation between theoretical values and experimental data as a function of angle β).

In the Lambert case, the fit of the theoretical shape to the data was fairly good, being in error by less than 6%. However, the nonrandom behavior of the deviation indicates that the overall shape of the Lambert analysis curve does not agree exactly with the data. Again, the percentage deviation varies in a systematic fashion when the Lommel-Seeliger analysis is used and the magnitude of deviation is much larger than for the Lambert analysis. Thus, the percent deviation indicates that the overall shape of the Lommel-Seeliger analysis does not approximate the data points. The percent deviation results for the Euler analysis indicates a similar nonrandom variation whose magnitude is greater than both the Lambert and Lommel-Seeliger analyses. Therefore, it appears as if the Euler analysis curve does not accurately describe the shape of the data. The last analysis used was the s factor. The essentially random percent deviation (Fig. 4) is small (much less than the Lommel-Seeliger and Euler analyses and slightly less for the Lambert analysis).

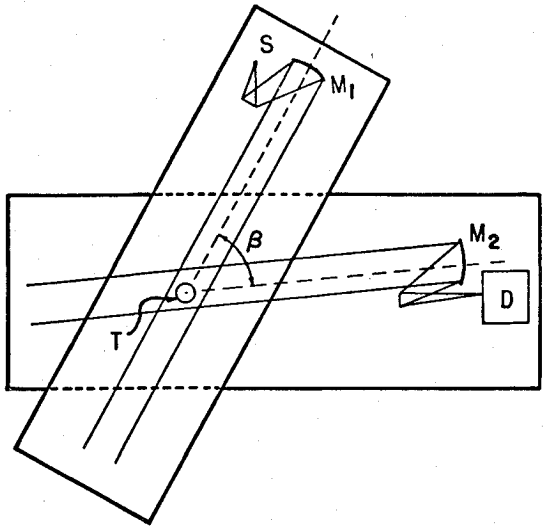

Fig. 1 Schematic of experimental apparatus.

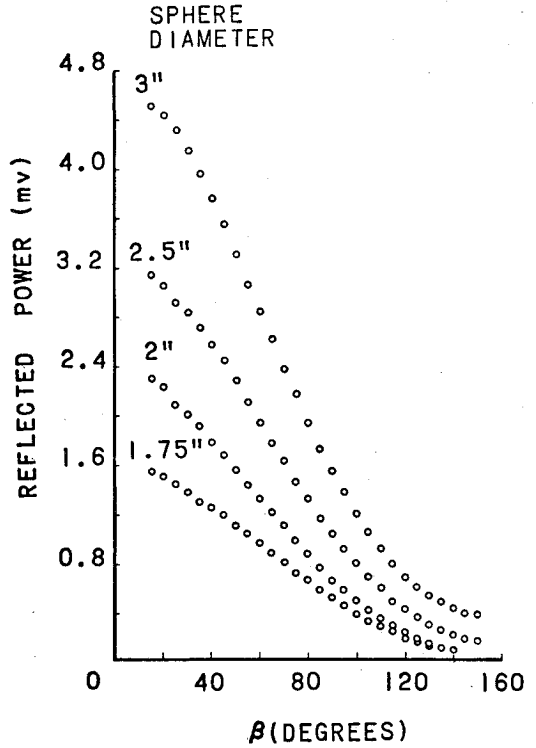

Fig. 2. Reflected power as a function of β (experimental).

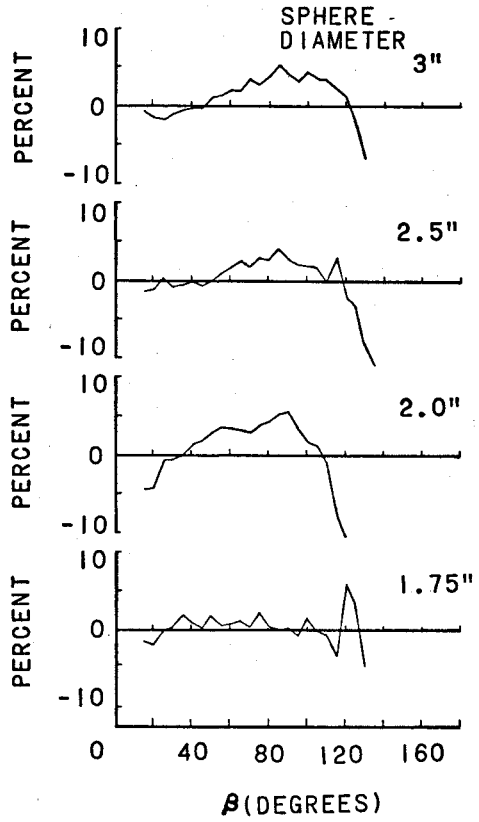

Fig. 3 Percent deviation between the theoretical values and experimental data as a function of β for the Lambert analysis.

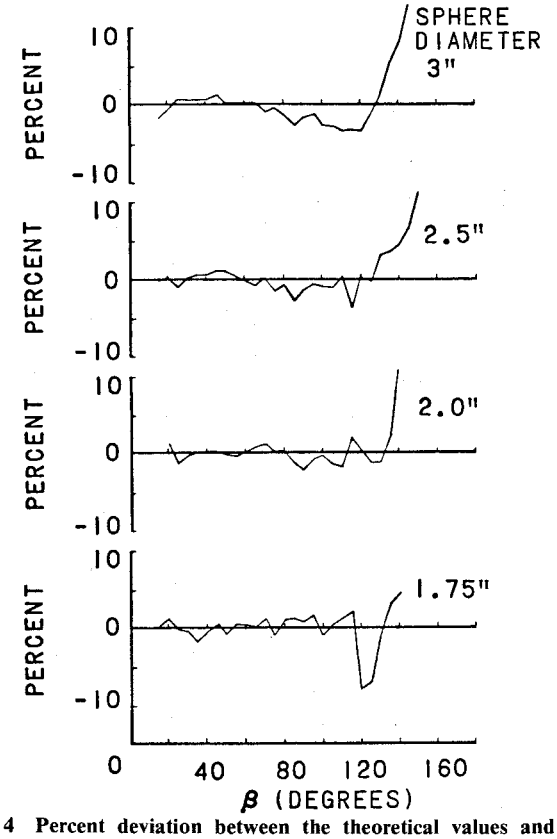

Fig. 4 Percent deviation between the theoretical values and experimental data as a function of β for the s factor analysis.

Conclusions

The reflectance models of Lommel-Seeliger and Euler do not accurately describe the power distribution upon reflection from the spheres. That is, the percentage deviation varies in a nonrandom fashion, thus the shape of the curves do not approximate the shape of the data.

The results do indicate that the classical Lambert analysis is a fair approximate model. But, because the theoretical values do deviate from the data (especially for the large spheres), it must be concluded that the Lambert curve shape does not fit the data curve exactly. However, the fit would probably be accurate enough for most engineering applications.

The s factor analysis does produce an adequate approximate model. The percentage deviation of the theoretical values and the data is less than 3%. The nonrandom deviation, however slight, indicates the s factor analysis cannot be said to describe the shape of the data exactly. However, the fit is well within the accuracy needed for engineering application.

References

[1] Rau, B. W. and Look, D. C., "Bibliography of Reflectance from Surfaces," University of Missouri-Rolla Report, Rolla Mo.. 1974.

[2] Russell, H.N., "On the Albedo of the Planets and Their Satellites," *Astrophyisical Journal,* Vol. 43, April 1916, pp. 43.

[3] Schoenberg, E., "Theorie Der Belenchtung Des Mondes Auf Grund Photometrischer Messungen," *Acta Societatis Scientiarum Fennicae,* Vol. 50, Sept. 1925.

[4] Look, D. C., Jr., "Diffuse Reflection from a Plane Surface," *Journal of the Optical Society of America,* Vol. 55, Dec. 1965, pp. 1628.

Some Comments on the Dirac-Delta Approximations for Chemical Reactions

K. Annamalai* and P. Durbetaki†
Georgia Institute of Technology, Atlanta, Ga.

Nomenclature

A	= preexponential factor
C	= coordinate compensation factor
c_p	= specific heat
D	= binary diffusion coefficient
$D_{III,g}$	= third Damköhler number
d	= diameter
E	= first exponential integral
E_g	= activation energy for gas phase oxidation
I,I'	= integral, Eqs. (3) and (4)
$\dot{m}$	= gasification rate
n	= overall order of reaction
n_i	= order of reaction with respect to species i
p	= pressure
Q	= heat of gasification
R	= gas constant
r	= radius
T	= temperature
W	= molecular weight
Y	= mass fraction
ϵ	= flux fraction
ξ	= dimensionless burning rate, $\dot{m}/4\pi\rho Dr$
η	= arbitrary coordinate
θ	= dimensionless temperature
θ_1,θ_2	= Eqs. (2b)

Received August 23, 1976.

Index categories: Reactive Flows; Combustion in Gases; Combustion in Heterogeneous Media.

*Graduate Research Assistant, Fire Hazard and Combustion Research Lab., School of Mechanical Engineering; presently Research Associate, Division of Engineering, Center for Fluid Dynamics, Brown University, Providence, R.I.

†Associate Professor, Fire Hazard and Combustion Research Lab., School of Mechanical Engineering.